

Synthesis and Characterization of Nanostructures: MWCNT_f/TiO₂ and MWCNT_f/TiO₂/HAp

C. Albano,^{*1,2} Y. Sarmiento,^{1,4} G. González^{*3,4}

Summary: In the present work nanostructured systems based on multiwalled carbon nanotubes (MWCNT) coated with titania (TiO₂), hydroxyapatite (HAp) and their combinations were synthesized using sol-gel and precipitation methods. Different synthesis variables were used (calcination, concentration of MWCNT and gel aging time). The TiO₂ nanoparticles size was 4.4 nm, independent of the synthesis conditions. The best coating was obtained by aging the gel during 20 days. Also the use of the surfactant SDS resulted in a good dispersion of the HAp particles on the MWCNT walls. HAp increases the thermal stability of MWCNTs.

Keywords: multiwall carbon nanotubes; nanocomposites; nanoparticles; structures

Introduction

Due to the excellent properties shown by nanomaterials, there has been the need for synthesizing different nanostructured materials for new applications. Multiwalled carbon nanotubes (MWCNTs) have been considered a good support for materials with catalytic and photocatalytic properties due to their large surface area, chemical stability and mesoporous character.^[1,2]

Therefore, it is possible to employ MWCNTs as support for TiO₂ nanoparticles and TiO₂-hydroxyapatite, obtaining a hybrid organic-inorganic material for numerous applications. In the present work, nanostructured composites MWCNT_f/TiO₂, MWCNT_f/HAp/TiO₂ and MWCNT_f/HAp were prepared.

Experimental Part

Oxidative Functionalization of MWCNTs

Functionalization of multiwalled carbon nanotubes^[3–5] was carried out in two stages, first prefunctionalization with nitric acid (HNO₃) and sulfuric acid (H₂SO₄) and then treatment under reflux with HNO₃ to obtain MWCNTs with carboxylic and hydroxyl groups (MWCNT_f).

Preparation of Nanocomposites

Nanostructured composites MWCNT_f/TiO₂, were prepared in two different concentrations (1:1 and 1:3) and two aging times (1 and 20 days). The synthesis of TiO₂ nanoparticles was carried out by sol-gel method,^[6–9] using titanium isopropoxide, isopropanol and acetic acid. For the nanostructured MWCNT_f/titania/HAp and MWCNT_f/HAp systems, HAp was synthesized, using calcium hydroxide, Ca(OH)₂, and ammonium phosphate, (NH₄)₂HPO₄,^[10] varying agitation time, temperature and addition of sodium lauryl sulfate (SDS) as surfactant. The nanostructured systems were labelled MWCNT_f/TiO₂(c)_{-Tc}.t; where c is the mass ratio of MWCNT/TiO₂, t is the aging time, Tc is the calcination temperature. The synthesis of nanostructured systems MWCNT_f/TiO₂/HAp was carried out with or without

¹ Escuela de Ingeniería Química, Facultad de Ingeniería, UCV, Caracas, Venezuela

² Laboratorio de Polímeros, Centro de Química, IVIC, Apdo. 21827, Caracas 1020-A, Venezuela
E-mail: carmen.albano@ucv.ve

³ Lab. de Materiales, Centro. Ing. Materiales y Nanotecnología; IVIC, Apdo. 21827, Caracas 1020-A, Venezuela

⁴ Escuela de Física, Facultad de Ciencias, UCV, Caracas, Venezuela
E-mail: gemagonz@ivic.gob.ve

surfactant. These samples were labeled $\text{MWCNT}_f/\text{TiO}_2(\text{c})_{-}\text{Tc}/\text{HAp}_{\text{tr.Tr.SDS}}$, where Tr and tr are the hydroxyapatite precursors reaction temperature and time.

Characterization of the Synthesized Nanostructured Systems

The characterization of all samples was carried out by Fourier transformed infrared spectroscopy (FTIR), in a Nicolet iS10 spectrometer with a resolution of 2 cm^{-1} . The XRD pattern was recorded using a diffractometer (Siemens, Model D 500) in the range of 20° – 60° . Thermal study was carried out in a thermogravimetric analyzer, Mettler Toledo TGA/SDTA 851e, from 25°C to 800°C with a heating rate of $10^\circ\text{C}/\text{min}$. Transmission electron microscopy (TEM) analysis was performed with a JEOL 2100, operating at 100 kV. The Brunauer, Emmett and Teller (BET) area method was used to measure superficial area with a Micromeritics (ASAP 2010) equipment.

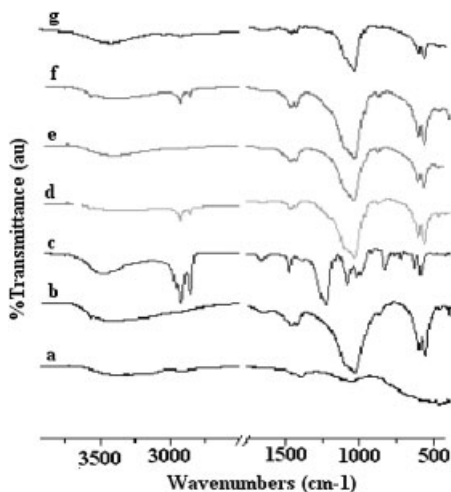


Figure 1.

FTIR spectra for nanostructured systems: a) $\text{MWCNT}_f/\text{TiO}_2(1:3)_{-}500^\circ\text{C}_{.20}$, b) HAp, c) surfactant SDS, d) $\text{MWCNT}_f/\text{TiO}_2(1:3)_{-}500^\circ\text{C}/\text{HAp}_{\text{Ta.30.SDS}}$, e) $\text{MWCNT}_f/\text{TiO}_2(1:3)_{-}500^\circ\text{C}/\text{HAp}_{\text{O}^\circ\text{C}_{.30}}$, f) $\text{MWCNT}_f/\text{TiO}_2(1:3)_{-}500^\circ\text{C}/\text{HAp}_{\text{O}^\circ\text{C}_{.30.SDS}}$ g) $\text{MWCNT}_f/\text{TiO}_2(1:3)_{-}500^\circ\text{C}/\text{HAp}_{\text{O}^\circ\text{C}_{.60.SDS}}$.

Results and Discussion

Figure 1 shows the FTIR spectra for the nanostructured composites $\text{MWCNT}_f/\text{HAp}$, $\text{MWCNT}_f/\text{TiO}_2$ and $\text{MWCNT}_f/\text{TiO}_2/\text{HAp}$, and also the HAp spectrum has been added for comparison. It can be observed that the nanocomposite with HAp shows similar bands to those of HAp, apart from the MWCNTs typical vibration bands. The nanostructured systems with TiO_2 , additionally to the MWCNTs vibration bands, show a very broad vibration band in the region 400 – 515 cm^{-1} , characteristic of the TiO_2 vibration (Figure 1a). Additionally, Figure 1 also shows the spectra for the materials prepared under different synthesis conditions: using surfactant (SDS), varying the synthesis temperatures and the aging periods. However, as can be seen, no significant differences are observed in these spectra, only the characteristic vibration bands of the different compounds are present, indicating that the variation in synthesis conditions does not change the interaction between the nanotubes and the nanoparticles.

Figure 2 presents the XRD patterns for the different nanostructured materials,

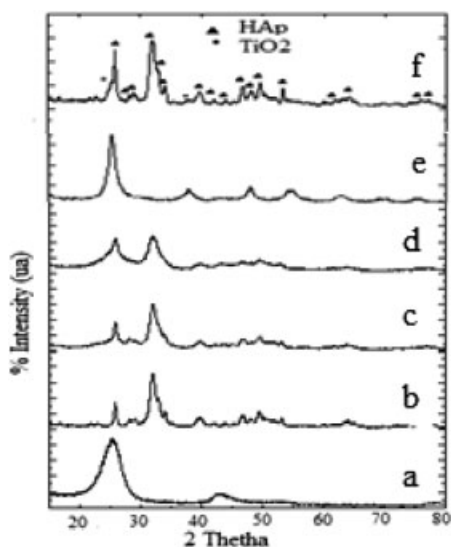


Figure 2.

XRD patterns: a) MWCNT_f , b) HAp, c) $\text{MWCNT}_f/\text{HAp}(1:3)$, d) $\text{MWCNT}_f/\text{HAp}(1:1)$, e) TiO_2 (anatase) f) $\text{MWCNT}_f/\text{TiO}_2(1:3)_{-}500^\circ\text{C}/\text{HAp}_{\text{Ta.30.SDS}}$.

MWCNT_f/HAp, MWCNT_f/TiO₂ and MWCNT_f/TiO₂/HAp, for different concentrations and different synthesis conditions. All the HAp reflections were identified in the MWCNT_f/HAp and for the TiO₂ composites, the anatase phase was obtained. An increase in the intensity is observed with the increase in HAp concentration (1:3). The particle size was calculated from the XRD patterns using the Scherrer equation, resulting in 6.3 nm for HAp crystallites and 4.4 nm for the TiO₂ compound. It is remarkable the effect of the MWCNTs on TiO₂ crystal size: when this compound was synthesized without the presence of nanotubes the crystal size was 272 nm, indicating a strong nucleation effect of the MWCNTs, as has been reported.^[10] Figure 2f corresponds to the XRD pattern of the nanostructured material MWCNT_f/TiO₂/HAp. As can be observed, the HAp reflections are much more intense than the TiO₂ reflections indicating that HAp is present in larger amount than TiO₂. It is possible that HAp has formed not only in the MWCNTs walls, but also as separated nanocrystals in the material, as has been observed by transmission electron microscopy. Figure 3 shows TEM images of the different nanostructured materials. It can be observed that the nanoparticles decorate the MWCNTs walls, however in the case of HAp composites, agglomerates of nanoparticles were also observed on mesh arrangements of MWCNTs (Figure 3). This explains the difference in intensity observed in the XRD patterns.

The average particle size of HAp measured from the TEM images was 7.6 nm and it was in a good agreement with the value obtained by XRD, with a rounded morphology. When HAp is synthesized without the presence of MWCNTs it has a bar morphology.^[12] For the nanocomposite MWCNT_f/TiO₂/HAp (Figure 3c), a mixture of nanoparticles of both compounds is observed on the MWCNTs walls.

TGA analyses of the different composites are shown in Table 1. It can be observed that the total weight loss is the largest for the MWCNT_f/TiO₂ composite, suggesting that HAp increases the thermal stability of these materials. The thermal degradation of these systems takes place in four stages. The first one from 32 °C to 103 °C corresponds to adsorbed water. The second and third stages correspond to the surfactant combustion. The structural water loss overlaps with these two stages. The last stage corresponds to the combustion of MWCNTs in the different systems. It is evident that the presence of HAp in the MWCNT_f/TiO₂ systems increases the oxidation temperature of the MWCNTs. A similar behavior is observed when the systems MWCNT_f/HAp, MWCNT_f/TiO₂ and MWCNT_f/TiO₂/HAp are compared, suggesting that a combination of TiO₂ and HAp shifts the combustion temperature of MWCNTs to higher temperatures, therefore increasing their thermal stability.

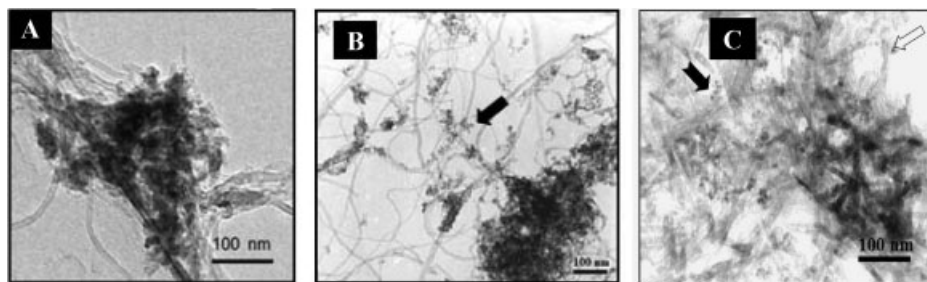


Figure 3.

TEM images of A) MWCNT_f/HAp, B) MWCNT_f/TiO₂ and C) MWCNT_f/TiO₂/HAp.

Table 1.Thermogravimetric analyses of MWCNT/TiO₂/HAp.

Nanostructured composites	Temperature (°C)	Minimum DTG (°C)	Remnant mass (%)
HAp	32–103	56	2.1
	103–430	196	9.1
	430–800	—	2.0
MWCNT _f /HAp(1.3)	35–116	64	2.4
	116–417	183	8.5
	417–745	—	26.2
MWCNT _f /TiO ₂ (1.3) _{500 °C.20}	33–128	65	4.4
	128–337	210	4.1
	370–740	—	25.4
MWCNT _f /TiO ₂ (1.3) _{500 °C/HAp_0 °C.60.SDS}	33–125	60	2.7
	125–260	216	4.6
	260–359	—	3.2
	359–460	405	2.6
	460–700	611	7.6

The superficial area of MWCNT_f/TiO₂ and MWCNT_f/TiO₂/HAp composites is very similar (141 cm²/g), almost twice the value of the superficial area of HAp (synthesized without nanotubes). This indicates the strong control effect of MWCNTs on HAp and TiO₂ crystal size.

Conclusion

For the composites MWCNT_f/TiO₂ the anatase phase was obtained with a crystallite size of ~4 nm. HAp on MWCNT_f has spherical morphology and a crystallite size of ~7 nm.

A reaction temperature of 0 °C and the use of SDS results in a more homogeneous coating of HAp on the MWCNT_f/TiO₂ composites compared to the system is synthesized at room temperature (≈25 °C) without the use of surfactant. The interaction of HAp with the composites increases the thermal stability of the MWCNTs.

- [1] H. Baughman, A. A. Zakhidov, W. A. De Heer, *Science* **2002**, 297, 787.
- [2] K. Byrappa, A. Dayananda, C. Sajan, B. Bsavalingu, M. Shayan, K. Soga, M. Yoshimura, *J. Mater. Sci.* **2008**, 47, 2348.
- [3] A. Hirsch, O. Vostrowsky, *Topics in Current Chemistry* **2005**, 193.
- [4] V. Datsyuk, M. Kalyva, K. Papagelis, J. Parthenios, D. Tasis, A. Siokou, I. Kallitsis, C. Galiotis, *Carbon* **2008**, 46, 833.
- [5] P.-H. Hou, C. Liu, H.-M. Cheng, *Carbon* **2008**, 46, 2003.
- [6] B. Gao, C. Peng, G. Z. Chen, G. Puma, *Applied Catalysis B: Environmental* **2008**, 85, 17.
- [7] R. A. Caruso, M. Antonietti, *Chemistry of Materials* **2011**, 13, 3272.
- [8] E. Gutiérrez, H. Pérez, J. Trejo, <http://148.206.53.231/UAM1289.PDF>
- [9] G. González, C. Albano, V. Hermán, I. Boyer, A. Monsalve, J. Brito, *Materials Characterization* **2012**, 64, 96.
- [10] S. Aryal, K. C. Remant, N. Dharmaraj, K.-W. Kim, H. Kim, *Scripta Materialia* **2006**, 54, 131.
- [11] Y. Yu, J. C. Yu, J.-G. Yu, Y.-C. Kwok, Y.-K. Che, J.-C. Zhao, W. K. Ding, *Applied Catalysis A: General* **2005**, 289, 186.
- [12] C. Albano, G. Gonzalez, C. Parra, *Polymer Bulletin* **2010**, 65, 893.